

Hypoxia Markers are Expressed in Interneurons Exposed to Recurrent Seizures

Fabio Gualtieri · Carla Marinelli · Daniela Longo ·
Matteo Pugnaghi · Paolo F. Nichelli ·
Stefano Meletti · Giuseppe Biagini

Received: 25 July 2012 / Accepted: 5 October 2012 / Published online: 17 October 2012
© Springer Science+Business Media New York 2012

Abstract An early but transient decrease in oxygen availability occurs during experimentally induced seizures. Using pimonidazole, which probes hypoxic insults, we found that by increasing the duration of pilocarpine-induced status epilepticus (SE) from 30 to 120 min, counts of pimonidazole-immunoreactive neurons also increased ($P < 0.01$, 120 vs 60 and 30 min). All the animals exposed to SE were immunopositive to pimonidazole, but a different scenario emerged during epileptogenesis when a decrease in pimonidazole-immunostained cells occurred from 7 to 14 days, so that only 1 out of 4 rats presented with pimonidazole-immunopositive cells. Pimonidazole-immunoreactive cells robustly reappeared at 21 days post-SE induction when all animals (7 out of 7) had developed spontaneous recurrent seizures. Specific neuronal markers revealed that immunopositivity to pimonidazole was present in cells identified by neuropeptide Y (NPY) or somatostatin antibodies. At variance, neurons immunopositive to parvalbumin or cholecystokinin were not immunopositive to pimonidazole. Pimonidazole-immunopositive

neurons expressed remarkable immunoreactivity to hypoxia-inducible factor 1 α (HIF-1 α). Interestingly, surgical samples obtained from pharmacoresistant patients showed neurons co-labeled by HIF-1 α and NPY antibodies. These interneurons, along with parvalbumin-positive interneurons that were negative to HIF-1 α , showed immunopositivity to markers of cell damage, such as high-mobility group box 1 in the cytoplasm and cleaved caspase-3 in the nucleus. These findings suggest that interneurons are continuously endangered in rodent and human epileptogenic tissue. The presence of hypoxia and cell damage markers in NPY interneurons of rats and patients presenting with recurrent seizures indicates a mechanism of selective vulnerability in a specific neuronal subpopulation.

Keywords Epilepsy · Hypoxia · Interneurons · Pharmacoresistance · Pilocarpine · Status epilepticus

Introduction

Seizures are generated by hyperactive neurons that require an adequate metabolic support in order to produce a sustained synchronized activation. It has been calculated that cerebral blood flow must increase over 200 % of basal levels to satisfy the demand of oxygen in cortical neurons during seizure activity (Kreisman et al. 1991). In principle, a failure in satisfying such an increased metabolic requirement could lead to neuronal cell death by ischemic/hypoxic mechanisms: this possibility has been suggested to explain lesions found in patients affected by temporal lobe epilepsy (TLE) (Plum et al. 1968; Simon 1985; Fabene et al. 2007). However, other authors (Meldrum and Nilsson 1976) demonstrated that cerebral blood flow and, consequently, oxygenation were both increased much over the required supply in epileptic animals.

Fabio Gualtieri, Carla Marinelli, and Daniela Longo equally contributed to the work.

Electronic supplementary material The online version of this article (doi:10.1007/s12017-012-8203-0) contains supplementary material, which is available to authorized users.

F. Gualtieri · C. Marinelli · D. Longo · G. Biagini (✉)
Dipartimento di Scienze Biomediche, Metaboliche e
Neuroscienze, Laboratorio di Epilettologia Sperimentale,
Università di Modena e Reggio Emilia, Via Campi 287,
41125 Modena, Italy
e-mail: gbiagini@unimore.it

M. Pugnaghi · P. F. Nichelli · S. Meletti
Dipartimento di Scienze Biomediche, Metaboliche e
Neuroscienze, Ospedale NOCSAE, Università di Modena e
Reggio Emilia, Via Giardini 1355, 41126 Modena, Italy

In line with this evidence, neuronal necrosis was found in several brain regions after short periods (25–45 min) of status epilepticus (SE) in animals with preserved oxygenation (Nevander et al. 1985; Ingvar 1986). These data along with the detection of excitotoxicity as the main mechanism responsible for neuronal cell death led to definitively abandon the cerebrovascular hypothesis of brain injury in epilepsy (Siesjö et al. 1986; Meldrum 2002).

Lines of evidence have recently renewed the interest on the cerebrovascular hypothesis. By using 4-aminopyridine, Zhao et al. (2009) showed that cerebral blood flow increases (+50 %) in response to ictal activity, as described before (Meldrum and Nilsson 1976), but only after an initial decrease (−23 %) in oxygen partial pressure. This activity-related hypoxia was found to be transient and limited to the epileptic focus, whereas the surrounding tissue was hyperoxygenated: two different phenomena that, by occurring concomitantly, have probably precluded the detection of hypoxia in many of the previous experiments. Similar evidence was also obtained in patients affected by pharmacoresistant epilepsy, in which an early increase in deoxygenated hemoglobin, matched by a reduction in oxygenated hemoglobin, closely occurred during the afterdischarge evoked by direct stimulation of the cerebral cortex (Ma et al. 2009). Even more intriguingly, the same laboratory has demonstrated that cortical hypoxia develops in a correlative manner in response to interictal discharges (Geneslaw et al. 2011). Overall, these data support the view that decreased oxygen availability occurs during ictal and interictal activation. Although these changes were not proven to damage the brain, hyperactive neuronal subpopulations could be selectively challenged.

Acute hypoxia is responsible for neuronal cell death, although mechanisms are still to be clearly defined (Hossain 2005; Northington et al. 2011). Chronic hypoxia has been associated with neuronal cell damage that is also dependent on neuroglobin oxidation and degradation, accumulation of ferric ions and release of cytochrome c, which finally triggers apoptosis (Hota et al. 2012). High-mobility group box 1 (HMGB1) is a nuclear protein loosely bound to the chromatin that plays an important role in cells undergoing apoptosis or necrosis (Scaffidi et al. 2002). In apoptotic cells, HMGB1 is tightly bound to chromatin and remains inside the nucleus. At variance, HMGB1 is released to the cytoplasm and, subsequently, secreted by cells exposed to *in vitro* hypoxia and glucose deprivation (Faraco et al. 2007) or to ischemia (Kim et al. 2006; Qiu et al. 2008), inducing an inflammatory reaction (cf. Yang et al. 2010). Lines of evidence suggest that hypoxia-inducible factor 1 α (HIF-1 α) may be an additional key mediator of neuronal death in chronic hypoxic conditions. HIF-1 α is regularly synthesized and metabolized by neurons in the presence of normal oxygenation (Semenza 2011). However, when neurons are exposed to hypoxia,

HIF-1 α is accumulated rather than degraded, and it could trigger a molecular cascade leading to apoptosis (Li et al. 2005, 2007; Chen et al. 2007; Yu et al. 2011).

Endogenous markers such as HIF-1 α (Rademakers et al. 2011), HMGB1 (Itoh et al. 2012), and the exogenous probe pimonidazole (Arteel et al. 1995; Noto et al. 2007; Thored et al. 2007) are currently used to reveal *in vivo* exposure to low oxygen levels. In particular, pimonidazole can readily diffuse in tissues, including the brain (Saunders et al. 1984), and it forms adducts with thiol groups in proteins, peptides, and amino acids of hypoxic cells, in such a way that this “hypoxyprobe” is retained and can be visualized by antibodies (Arteel et al. 1998; Kizaka-Kondoh and Konse-Nagasawa 2009). A possible advantage of these molecular probes is that they could reveal the presence of cell populations particularly vulnerable to short episodes of hypoxia. Thus, we used these markers to investigate whether hypoxia develops in the presence of spontaneous seizures, such as those observed in the pilocarpine model (Curia et al. 2008). Furthermore, we aimed at assessing whether hypoxia could be associated with cell suffering. In order to address these hypotheses, we designed a series of experiments in rats to evaluate whether: (1) increasing duration of pilocarpine-induced SE promotes the appearance of pimonidazole-immunopositive cells; (2) immunoreactivity to pimonidazole varies during a time course of 3 weeks after SE, thus going through the latent period up to the appearance of spontaneous seizures; (3) specific neuronal subclasses could be identified by pimonidazole; (4) neurons presenting immunopositivity to pimonidazole also express markers of damage. Finally, (5) we aimed at establishing a parallelism with the animal model in human tissue from pharmacoresistant patients by assessing whether neurons within the epileptogenic zone presented with anomalous HMGB1 immunoreactivity or expressed HIF-1 α as well as cleaved caspase-3.

Methods

Animals and Treatments

Adult male Sprague–Dawley rats (Harlan, S. Pietro al Natisone, UD, Italy), weighing 230–250 g, were used ($n = 68$). All experiments were conducted in accordance with the European Directive 2010/63/EU and approved by the Italian Ministry of Health. We designed two different experiments, in which 63 rats were pretreated with methylscopolamine (1 mg/kg, *i.p.*; Sigma-Aldrich, Milan, Italy) to prevent the peripheral effects of cholinergic stimulation (Curia et al. 2008), and after 30 min, they were injected with *i.p.* pilocarpine (380 mg/kg) to induce SE. In the first experiment, rats were killed 30, 60, and 120 min after the

Table 1 The design of experiments based on the pilocarpine model is illustrated

	Experimental groups					
	I	II	III	IV	V	VI
SE (min)	30	60	120	30	30	30
Killing (days)	0	0	0	7	14	21
Sample size (<i>n</i>)	6	4	4	5	4	7

Rats were killed acutely (groups I–III), during the latent period (groups IV–V) or in the chronic period (group VI) of the pilocarpine model (Curia et al. 2008). Status epilepticus (SE) induced by pilocarpine (380 mg/kg) was limited by injecting diazepam (20 mg/kg) after 30 min from the onset, in groups IV–VI (Biagini et al. 2008; cf. Gualtieri et al. 2012)

onset of SE. In the second experiment, diazepam (20 mg/kg i.p.) was used to quell seizure activity after 30 min of SE and rats were then killed 7, 14, and 21 days after the pilocarpine treatment (Gualtieri et al. 2012). Rats in the second experiment were monitored continuously for 6 h following treatments and motor seizures completely disappeared within this time interval. We considered SE as the stage in which rats did not recover normal behavior (i.e., exploration, grooming, or motor reaction to stimuli) between one seizure and the other. This stage was usually reached after 3 stage 5 seizures (cf. Gualtieri et al. 2012). In general, seizure activity during SE did not stop for more than 1 min. To monitor the appearance of spontaneous recurrent seizures, rats were video recorded 6 h/day until killing, as previously described (Biagini et al. 2006, 2008). Seizures were graded according to a modified Racine's scale (Racine 1972; Biagini et al. 2008). The experimental design is shown in Table 1. An additional 5 rats were treated with saline and considered as controls.

To assess hypoxia, rats (controls, $n = 5$; pilocarpine, $n = 28$) were injected with pimonidazole (60 mg/kg, i.p.; HypoxyprobeTM, Hypoxyprobe Inc., Burlington, MA, USA) and, 15 min later, anesthetized with chloral hydrate (450 mg/kg, i.p.). Two pilocarpine-treated rats which developed spontaneous recurrent seizures were saline-injected and used as negative controls for the pimonidazole antibody. When deeply anesthetized (approximately 15 min after chloral hydrate injection), rats were perfused via the ascending aorta with 100 ml saline followed by 100 ml (10 ml/min) 4 % paraformaldehyde and picric acid (0.3 %) dissolved in 0.1 M phosphate buffer (pH 6.9). Brains were then postfixed overnight in the same fixative at 4 °C and, after cryoprotection by immersion in 15 and 30 % sucrose-phosphate buffer solutions, were frozen and cut horizontally with a freezing microtome in serial 50- μ m-thick sections, subsequently used for immunohistochemistry.

Surgical Specimens

Six patients with focal drug-resistant epilepsy underwent to a tailored cortectomy after non-invasive presurgical

protocol. All subjects were seizure-free at the last follow-up (16–42 months; median: 30 months). An anterior temporal cortectomy, including the amygdala and hippocampus, was performed in three patients; a frontal lobe cortectomy was performed in the other three subjects (Table 2). Tissue samples were postfixed for 3 days in the previously described fixative, then cryoprotected. Samples were cut by a cryostat in 40- μ m-thick sections and processed for immunofluorescence.

Immunohistochemistry

In order to evaluate neurons positive to the pimonidazole antibody (Table 3), sections from rat brains were processed for immunohistochemistry with the avidin–biotin complex (ABC) technique, using diaminobenzidine as chromogen (Biagini et al. 2008). Then, to identify the nature of pimonidazole-positive cells, we performed double-staining immunofluorescence experiments with antibodies specific for different classes of interneurons (Table 3). Similar double-staining experiments were performed on the human specimens, in order to identify the presence of immunoreactivity for HIF-1 α . Antibodies for hypoxia, cell damage, and apoptosis are reported in Table 3. Free-floating sections were washed in phosphate-buffered saline (PBS) at room temperature and permeabilized for 1 h in PBS containing 0.1 % Triton X-100 and 1 % bovine serum albumin. For double immunolabelling, sections were incubated overnight in a mixture of mouse monoclonal IgG and a rabbit polyclonal antibody. For the characterization of different cellular subtypes, we used specific rabbit polyclonal antibodies reported in Table 3. After washing, sections were incubated for 90 min at room temperature in a 1:200 dilution of goat anti-mouse AlexaFluor546[®] and goat anti-rabbit AlexaFluor488[®] (Invitrogen, Carlsbad, CA, USA). Sections were counterstained with 4',6-diamidino-2-phenylindole (DAPI, Vector Laboratories, USA) to assess nuclear morphology. Images were visualized using a Leica TCS SP2 confocal microscope, equipped with Argon (488 nm) and Helium/Neon (543 nm).

Table 2 Demographics, electroclinical features, and pathology of pharmacoresistant patients

Pt	Age/ gender	Epi	Seizure types	Seizures before surgery	Age of epi onset	Cortectomy	Pathology	Surgery outcome (Engel class)
P1	44/f	Symptomatic	FLE Hypermotor seizures in sleep	>10	8	Medial pre-frontal cortex	FCD type IIb	Ia
P2	49/f	Medial	TLE Arrest, oral automatism, postictal aphasia	2	17	Anterior temporal lobectomy	DNET of fusiform and parahippocampal gyrus + HS	Ia
P3	20/m	Symptomatic	FLE Arrest, fear, then tonic posturing of the right foot	>5	17	Lateral and medial prefrontal cortex	Gliosis	Ia
P4	44/m	Medial	TLE Hypermotor seizure in sleep	>10	22	Anterior temporal lobectomy	DNET of the amygdala and parahippocampal gyrus + HS	Ia
P5	32/m	Medial	TLE Arrest, oral automatism	1	17	Anterior temporal lobectomy	HS	Ia
P6	16/m	Symptomatic	FLE Hypermotor seizures in sleep	3	3	Medial pre-frontal cortex	FCD type IIb	Ia

Seizures scored during the week preceding the surgical intervention are indicated. Focal cortical dysplasia (FCD) was classified according to Blümcke et al. (2011). DNET dysembryoplastic neuroepithelial tumor, Epi epilepsy, f female, FLE frontal lobe epilepsy, HS hippocampal sclerosis, m male, Pt patient code, TLE temporal lobe epilepsy

Image Analysis

Sections stained by the ABC technique were evaluated at the microscope (Axioskop, Carl Zeiss Vision GmbH, München, Germany) and the positively immunostained regions were uploaded using a Sony CCD-IRIS B–W video camera in 6 serial sections separated by 0.75 mm, for each rat. Images were then analyzed by the KS300 image analysis software (Carl Zeiss Vision GmbH), as previously detailed (Biagini et al. 2008; Gualtieri et al. 2012). Background values were obtained from areas that did not contain any stained cell. Specifically immunostained cells were identified throughout every sampled region after statistical discrimination by setting a threshold obtained by subtracting the double value of standard deviation from the mean value of gray profiles (Biagini et al. 1993, 2005, 2006). Then, immunopositive cells were determined in each field as the number of objects, automatically transformed in D-circles (i.e., in circles having the same area of the identified objects) and counted by considering a minimum cutoff value of 7 μm for cell diameter. Cell counts were then divided by the sampled area and expressed as cell densities. Sampled areas were: nucleus accumbens (Acb, including core and shell regions); amygdala (Amg); caudate putamen (CPu); external cortex of the inferior colliculus (ECIC); interpeduncular nucleus—rostral subnucleus (IPR); paraventricular hypothalamic nucleus (PVH); dorsal raphe and tegmental nucleus (Tg, including laterodorsal Tg and peduncolopontine Tg).

Statistical Analysis

Statistical comparisons for pilocarpine experiments were performed by two-way analysis of variance (ANOVA; time was the between factor and sampled brain regions were the within factor) using SigmaPlot 11 (Systat Software, San Jose, CA, USA). The Fisher's Least-Significant-Difference (LSD) was used for post hoc comparisons. Values are presented as mean \pm SEM; $P < 0.05$ was chosen as threshold for significant differences.

Results

Distribution of Pimonidazole Immunoreactivity After Pilocarpine-Induced SE

We addressed the hypothesis that neurons could be exposed to hypoxia during seizure activity by characterizing the distribution of immunoreactivity for pimonidazole after pilocarpine-induced SE, in comparison with control non-epileptic rats (Supplementary Figure 1). To this purpose, we administered the hypoxyprobe pimonidazole to three

Table 3 Antibodies used in immunofluorescence experiments

Antibodies	Source	Isotype	Clone	Code	Dilution	Supplier
Parvalbumin	Rabbit	IgG		Ab11427	1:2,000	Abcam, Cambridge, MA, USA
Parvalbumin	Mouse	IgG		McAB 235	1:2,000	Swant, Bellinzona, Switzerland
Neuropeptide Y	Mouse	IgG	F-6	Sc-133080	1:250	Santa Cruz Biotechnology, Santa Cruz, CA, USA
Neuropeptide Y	Rabbit	IgG		T-4070	1:250	Peninsula Bachem Weil AM, Rhein, Germany
Somatostatin-28	Rabbit	IgG		20089	1:250	Immunostar, Hudson, WI, USA
Hypoxia-inducible factor 1 α	Rabbit	IgG		NB100-479	1:500	Novus Biologicals, Cambridge, UK
Hypoxia-inducible factor 1 α	Mouse	IgG	H1 α 67	MAB 5382	1:500	Millipore, Billerica, MA, USA
High-mobility group box 1	Rabbit	IgG		AB18256	1:500	Abcam, Cambridge, MA, USA
Cleaved caspase-3	Rabbit	IgG	Asp175	9661	1:20,000	Cell Signaling, Danvers, MA, USA
Hypoxyprobe mab-1	Mouse	IgG	4.3.11.3	90204	1:50	Millipore, Billerica, MA, USA
Cholecystokinin-8	Rabbit	IgG		20078	1:500	Immunostar, Hudson, WI, USA

In co-labeling experiments with the anti-pimonidazole antibody (hypoxyprobe), polyclonal antibodies were used to identify the other respective marker

different groups of rats that were killed 30 min ($n = 6$), 60 min ($n = 4$), and 120 min ($n = 4$) after the onset of SE. In these animals, we noticed the presence of three different patterns of immunostaining. The first one consisted of diffuse interstitial immunopositivity, similar to that described by others in models of cerebral ischemia (Noto et al. 2006, 2007; Thored et al. 2007). These areas were especially pronounced in the hippocampus (cornu Ammonis, CA), dentate gyrus (DG), parasubiculum (PaS), CPu, Acb, Tg, and DR (arrows in Fig. 1a), as identified after counterstaining with toluidine blue (Supplementary Figure 2). The second pattern of immunostaining, instead, consisted of the presence of isolated Golgi-like stained neurons identified by anti-pimonidazole antibodies in several brain regions (inset in Fig. 1a and arrows in Fig. 1b). Finally, a third pattern of immunostaining was localized only in mesopontine structures, and it was represented by intensely positive neuronal somas found in IPR, DR, and Tg (not magnified in Fig. 1, cf. Fig. 2c), remembering the distribution of the immunostaining reported in a model of cerebral malaria (Hempel et al. 2011). On the other hand, pimonidazole immunopositivity was lacking in control non-epileptic rats (Supplementary Figure 1). Neuronal cell counts of positive somas and of Golgi-like immunostained cells revealed that the immunoreactivity for pimonidazole increased significantly in specific brain regions ($F = 5.13$; $P < 0.01$ two-way ANOVA) and by varying the duration of SE ($F = 14.57$; $P < 0.01$ two-way ANOVA), without a significant interaction between the considered factors (Fig. 1c). In particular, immunopositive cells significantly increased in the CPu ($P < 0.01$, 120 vs 60 min), DR and Tg (for both regions, $P < 0.05$, 120 vs 30 min) of rats exposed to 120 min of SE. Furthermore, immunostained cells appeared de novo in ECIC and PVH of rats exposed to 120 min of SE (Fig. 1c). These findings suggested that

induction of pimonidazole immunopositivity in the pilocarpine model was seizure-dependent.

Distribution of Pimonidazole Immunoreactivity During the Latent Period and in Rats with Spontaneous Seizures

In order to challenge the hypothesis that induction of pimonidazole immunoreactivity was not due to the pilocarpine injection but, alternatively, to seizures, we examined the time course of counts of pimonidazole-immunoreactive cells in rats surviving to SE and then developing spontaneous recurrent seizures (Fig. 2). Animals were video monitored as previously described (Biagini et al. 2006, 2008), starting 1 day after SE. Rats were killed 7 days ($n = 5$), 14 days ($n = 4$), and 21 days ($n = 7$) after induction of SE. In rats killed 1 week after SE, we observed spontaneous seizures in 2 out of 5 rats just 24 h after SE induction, but not in the following days. In these animals, we did not observe the pattern of diffuse immunostaining observed in rats killed during SE, but anti-pimonidazole antibodies identified the presence of Golgi-like stained cells in at least one cerebral region of all the animals. In particular, pimonidazole-immunopositive cells were always detected in the CPu, whereas only 1 out of 5 rats presented immunoreactive cells in the Amg and PVH (Fig. 2d).

No seizures were observed in rats killed 2 weeks after the pilocarpine injection. However, seizures may have occurred outside of video recording periods. With the only exception of 1 out of 4 animals, all other rats from this group did not present with pimonidazole-immunoreactive cells. The animal that displayed Golgi-like immunostained cells and intensely positive somas for pimonidazole presented immunoreactivity in Acb, CPu, ECIC, and IPR (Fig. 2d). It has to be noted that this rat had an anomalous,

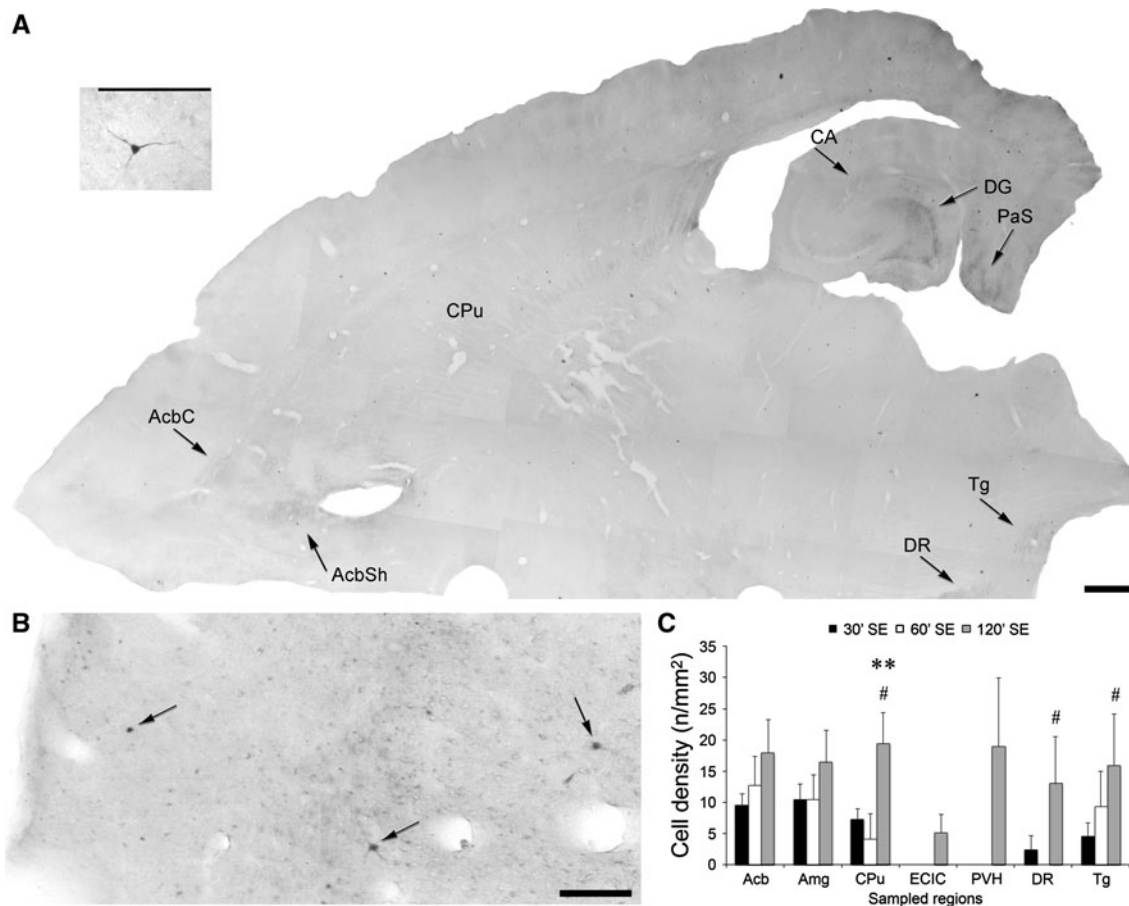


Fig. 1 Changes in pimonidazole-immunopositive cells in response to increasing periods of status epilepticus (SE). Rats were killed after 30, 60, or 120 min after the onset of SE. Two different patterns of immunostaining are illustrated in these photomicrographs, whereas a third pattern is shown in Fig. 2c. Specifically, in **a** arrows point to a diffuse immunostaining that do not allow to identify any specific cellular structure, in areas such nucleus accumbens (Acb, including core and shell regions, magnified in **b**), caudate putamen (CPU), cornu Ammonis (CA), dentate gyrus (DG), dorsal raphe (DR), parasubiculum (PaS) and tegmental nucleus (Tg, including laterodorsal Tg and pedunculopontine Tg). At variance, pimonidazole-immunopositive

darkly stained cells, often resembling Golgi-like neurons (inset in **a** and arrows in **b**) were observed in several brain regions and counted when they appeared particularly consistent. In **c**, neuronal cell counts of pimonidazole-immunopositive cells demonstrate a significant increase in rats exposed to 120 min of SE, as well as the appearance of immunopositive cells in the external cortex of the inferior colliculus (ECIC) and the paraventricular hypothalamic nucleus (PVH), that were absent with shorter time intervals from the SE onset. $**P < 0.01$ versus the group exposed to 60 min of SE, $\#P < 0.05$ versus the group exposed to 30 min of SE, Fisher's LSD test. Scale bars, 500 and 200 μm , respectively, for **a** and **b**

lethal reaction to anesthesia prior to perfusion, so we cannot exclude that this event could have affected immunoreactivity to pimonidazole. However, the comparison of rats killed 1 week after the SE with those killed a further week later clearly showed a decline of the immunopositivity to pimonidazole.

At the end of the third week of video monitoring, all rats (7 out of 7) belonging to the group killed 3 weeks after SE had developed spontaneous recurrent seizures classified as stage 5 of Racine's scale (Racine 1972). In this group, seizures were observed in 4 rats the same day of killing, or 2, 7, and 10 days before the pimonidazole injection in, respectively, the remaining animals. One of the animals that had seizures the same day of killing, along with the rat that presented with seizures 10 days before, were not injected with

pimonidazole and used as negative controls for the immunostaining. Apart from these rats and the control non-epileptic group, which did not present immunoreactivity for pimonidazole (Supplementary Figure 1), pimonidazole-immunopositive cells were present in various brain regions of all spontaneous epileptic animals (Fig. 2a–c, cf. Supplementary Figure 3), specifically in Acb, Amg, CPU, ECIC, IPR, PVH, DR, Tg (Fig. 2d). Sparse cells were noticed, but not counted, in other brain regions, such as the cerebral neocortex, insular, perirhinal and entorhinal cortices, and CA. No evidence of diffuse immunostaining, reminiscent of ischemic-like lesions (Noto et al. 2006, 2007; Thored et al. 2007), was found in any rat of this group. Although neuronal counts were similar in regions such as Acb, Amg, and ECIC, a non-significant trend toward a decrease was present in the

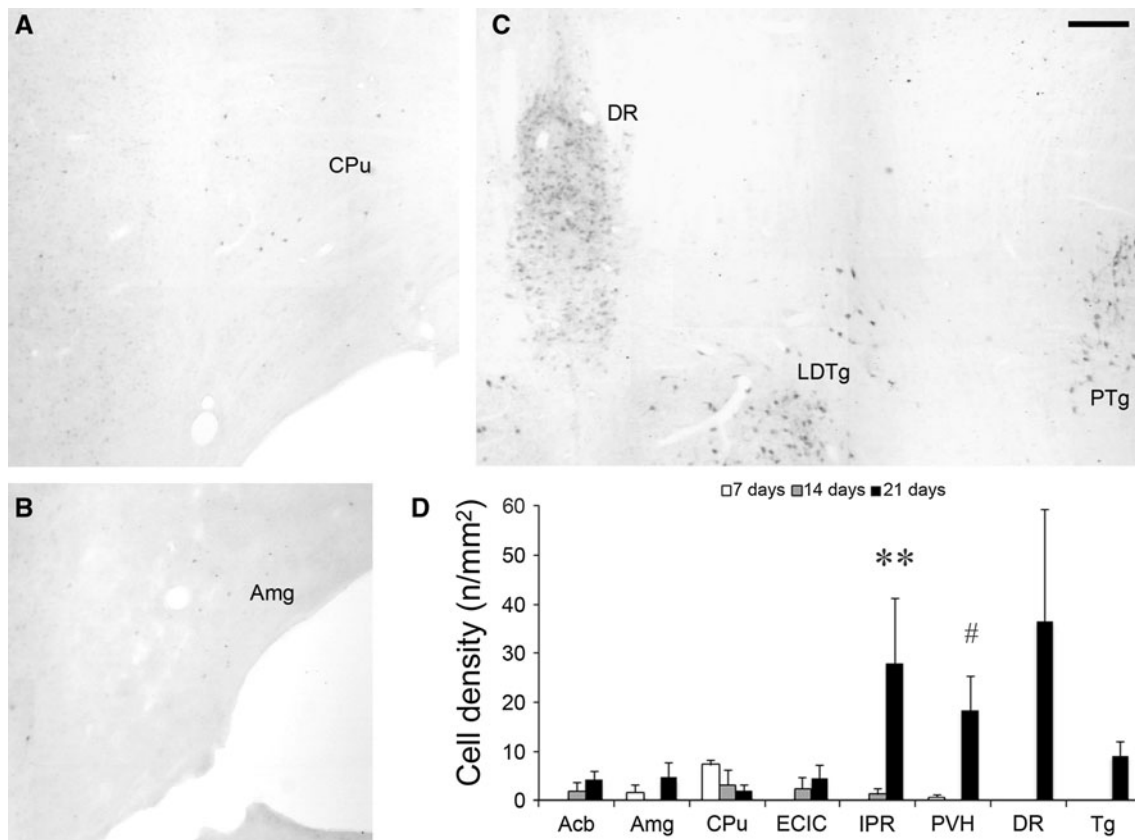


Fig. 2 Time course of the changes in pimonidazole-immunopositive cells after status epilepticus (SE). Rats were killed after 7, 14, or 21 days after the onset of SE, which was limited to 30 min by injecting diazepam (20 mg/kg). Two different patterns of immunostaining were found in these animals: the anti-pimonidazole antibody stained sparse cells with dendritic processes well delineated, thus appearing as Golgi-like neurons (a and b, cf. Fig. 1a), or grouped cells just stained in somas (shown in c). Cell counts in nucleus accumbens (Acb, including core and shell regions), amygdala (Amg),

caudate putamen (CPu), external cortex of the inferior colliculus (ECIC), interpeduncular nucleus—rostral subnucleus (IPR), paraventricular hypothalamic nucleus (PVH), dorsal raphe (DR) and tegmental nucleus (Tg, including laterodorsal Tg and pedunculopontine Tg) revealed significant increase of pimonidazole-immunopositive darkly stained cells in rats killed 3 weeks after SE (d). ** $P < 0.01$ versus the group killed after 14 days, # $P < 0.05$ versus the group killed after 7 days, Fisher's LSD test. Scale bar, 200 μ m

CPu of rats killed 7, 14, or 21 days after SE (Fig. 2d). More interestingly, a significant ($F = 8.81$; $P < 0.01$, two-way ANOVA) difference was found by comparing the various time intervals considered in this study. A remarkable increase in pimonidazole-immunopositive cells was observed in IPR ($P < 0.01$, 21 vs 14 days) and PVH ($P < 0.05$, 21 vs 7 days) of rats killed 3 weeks after SE, in which pimonidazole-immunopositive cells also appeared de novo in DR and Tg. These findings demonstrate that pimonidazole immunoreactivity was present in rats presenting with spontaneous seizures 3 weeks after the induction of SE, suggesting that it was related to the epileptic activity.

Identification of Pimonidazole-Immunopositive Neurons

We tried to identify the nature of cells presenting with Golgi-like immunostaining. As they appeared as isolated

cells in most of the pimonidazole-immunopositive brain regions, we hypothesized that they could be interneurons. To this aim, in rats killed 3 weeks after the SE, we performed double labeling with antibodies directed against parvalbumin (PV), neuropeptide Y (NPY), cholecystokinin (CCK), and somatostatin. These experiments demonstrated that PV did not co-localize with the anti-pimonidazole antibody (Fig. 3a). At variance, we found that pimonidazole-immunopositive cells were frequently, although not exclusively, expressing NPY immunofluorescence (Fig. 3b). Further experiments demonstrated that also somatostatin antibodies co-localized with pimonidazole in interneurons (Fig. 3c), whereas cells stained with anti-CCK antibodies were not immunopositive to pimonidazole (Fig. 3d). These experiments clearly identified NPY and somatostatin interneurons as expressing pimonidazole adducts in spontaneous epileptic rats. In particular, 14 % of somatostatin interneurons were immunopositive to

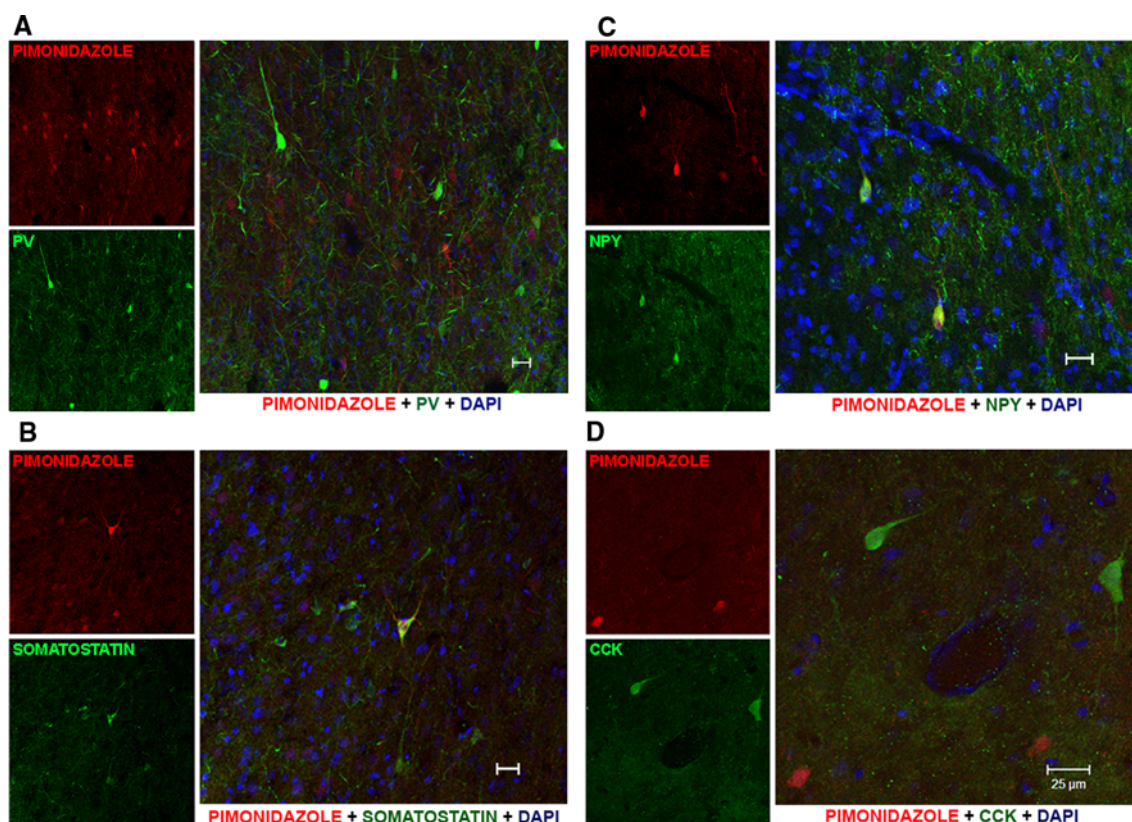


Fig. 3 Photomicrographs illustrating localization of pimonidazole immunopositivity in interneurons of pilocarpine-treated rats, studied 3 weeks after induction of status epilepticus. Interneurons were, respectively, identified by anti-parvalbumin (*PV*), anti-somatostatin, anti-neuropeptide Y (*NPY*), or anti-cholecystokinin (*CCK*) antibodies.

Note that anti-*NPY* and anti-somatostatin antibodies, but not the other antibodies, co-localize with pimonidazole-immunopositive cells. Photomicrographs were obtained from entorhinal and perirhinal cortices (*PV*, *NPY* and somatostatin) or from the hilus of dentate gyrus (*CCK*) of different rats. Scale bars, 25 μ m

pimonidazole antibodies, whereas 40 % of *NPY* interneurons co-expressed pimonidazole immunofluorescence.

HIF-1 α as a Marker of Hypoxia in Patients Affected by Pharmacoresistant Epilepsy

We asked whether evidence similar to that found in spontaneous epileptic rats could be found in patients affected by pharmacoresistant epilepsy. In this case, we did not use pimonidazole in patients for ethical reasons, but we decided to evaluate the presence of HIF-1 α in interneurons as a putative marker of exposure to hypoxia. As shown in Fig. 4, all (100 %) pimonidazole-immunopositive neurons in rats were co-labeled by antibodies against HIF-1 α , suggesting that HIF-1 α is accumulated in the same neurons presenting with pimonidazole adducts in rats with spontaneous seizures. Then, by evaluating HIF-1 α immunoreactivity in surgical specimens of patients affected by pharmacoresistant epilepsy, we found that interneurons immunopositive to *NPY* antibodies also expressed HIF-1 α immunoreactivity. Approximately 57 % of interneurons positive to *NPY* antibodies were co-stained by HIF-1 α

antibodies. At variance, *PV*-immunopositive interneurons were negative to HIF-1 α antibodies (Fig. 5). These findings suggest the possibility that episodes of hypoxia could involve *NPY*-positive interneurons in patients affected by pharmacoresistant epilepsy, as found in pilocarpine-treated rats.

Interneurons Expressing HIF-1 α Immunoreactivity Present Evidence of Cell Damage

We also tried to explore the possibility that interneurons expressing HIF-1 α immunoreactivity in patients affected by pharmacoresistant epilepsy could also present immunoreactivity for markers of cell damage. To this aim, we used an antibody against HMGB1, a protein that is known to be released from nuclei to the cytoplasm and, subsequently, secreted by cells exposed to ischemia (Kim et al. 2006; Qiu et al. 2008; reviewed by Yang et al. 2010). As shown in Fig. 6, evidence for translocation of HMGB1 from neuronal nuclei to the cytoplasm was found in both *PV*- and *NPY*-immunopositive interneurons of patients affected by pharmacoresistant epilepsy. Interneurons

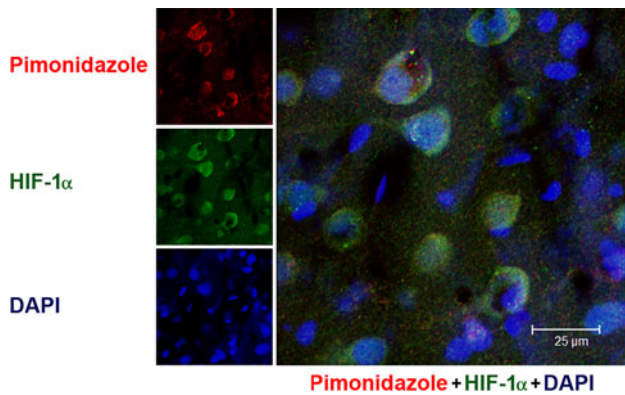


Fig. 4 Photomicrographs illustrating the distribution of hypoxia-inducible factor 1 α (*HIF-1 α*) immunoreactivity in cells identified by the anti-pimonidazole antibody. The immunolabelling was done on pilocarpine-treated rats, studied 3 weeks after induction of status epilepticus. Photomicrographs were obtained from the perirhinal cortex. Note that all pimonidazole-immunopositive cells also express *HIF-1 α* fluorescence. *Scale bar*, 25 μ m

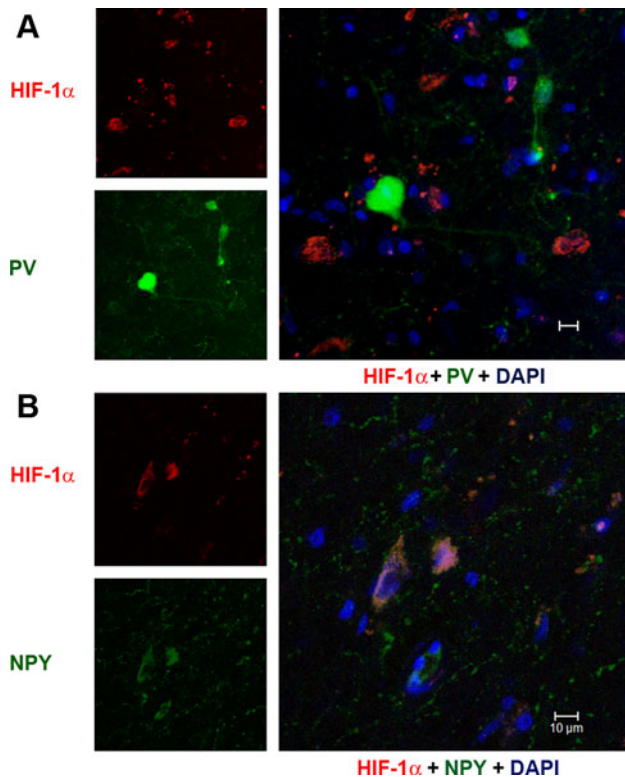


Fig. 5 Photomicrographs illustrating localization of hypoxia-inducible factor 1 α (*HIF-1 α*) immunopositivity in interneurons of patient P2 (Table 2), affected by temporal lobe epilepsy. Interneurons were, respectively, identified by anti-parvalbumin (*PV*) and anti-neuropeptide Y (*NPY*) antibodies. Note that interneurons immunopositive for *NPY* co-express immunofluorescence for *HIF-1 α* . *Scale bars*, 10 μ m

presenting with HMGB1 immunoreactivity in the cytoplasm were, respectively, 60 and 20 % of *NPY*- and parvalbumin-immunopositive cells. These results suggest that

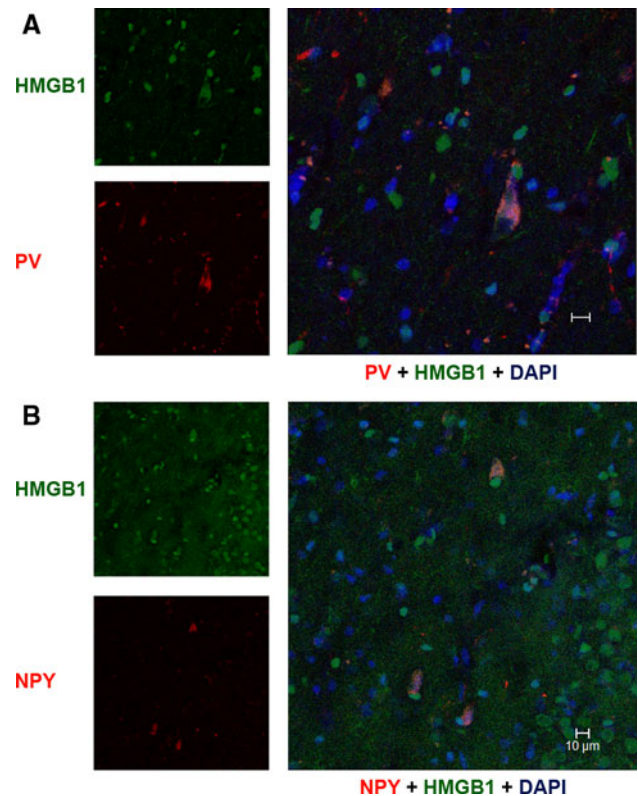


Fig. 6 Photomicrographs illustrating localization of high-mobility group box 1 (*HMGB1*) immunopositivity in interneurons. Interneurons were, respectively, identified by anti-parvalbumin (*PV*) and anti-neuropeptide Y (*NPY*) antibodies. These photomicrographs are from patient P4 (Table 2), affected by temporal lobe epilepsy. Note that interneurons immunopositive for both *PV* and *NPY* co-express immunofluorescence for *HMGB1*. *Scale bars*, 10 μ m

damage to *NPY* interneurons, which were previously shown to be immunopositive to *HIF-1 α* , as well as to *PV* interneurons occurred in the brain of patients undergoing the surgical treatment.

To further assess damage in *NPY* and *PV* interneurons, we evaluated the presence of cleaved caspase-3, a marker of apoptosis, in the cerebral samples obtained from patients affected by pharmacoresistant epilepsy. Caspase-3 is cleaved (activated) in the cytoplasm and then translocated into the nucleus. This phenomenon is very rapid and cleaved caspase-3 is only transiently found in cytoplasm after cerebral ischemia, before it moves in the nuclear region (Cao et al. 2001). In particular, we assessed the possible co-localization of cleaved caspase-3 with markers of interneuronal subpopulations. As shown in Fig. 7, both *PV* and *NPY* interneurons were found to present immunoreactivity for cleaved caspase-3, a finding consistent with experiments on surgical specimens from patients affected by TLE (Henshall et al. 2000; Schindler et al. 2006).

Finally, we investigated the presence of *HIF-1 α* and cleaved caspase-3 immunofluorescence in brain specimens

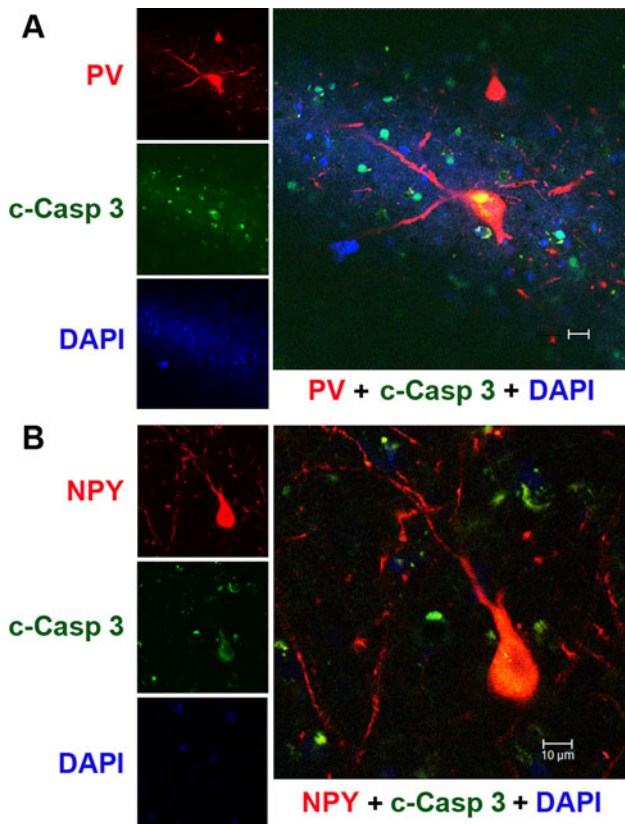


Fig. 7 Photomicrographs illustrating localization of cleaved caspase 3 (*c-Casp 3*) immunofluorescence in interneurons. Interneurons were, respectively, identified by anti-parvalbumin (*PV*) and anti-neuropeptide Y (*NPY*) antibodies. These photomicrographs are from patient P4 (Table 2), affected by temporal lobe epilepsy. Note that interneurons immunopositive for both *PV* and *NPY* co-express immunofluorescence for *c-Casp 3*. Scale bars, 10 μ m

of patients affected by pharmaco-resistant epilepsy (Fig. 8). We found that approximately all HIF1 α -immunopositive cells (89 %) also expressed cleaved caspase-3 immunoreactivity, whereas some cleaved caspase-3-immunopositive cells were not labeled by HIF-1 α antibodies.

Discussion

We have designed a series of experiments in order to assess whether neurons could be exposed to hypoxia in the presence of recurrent seizures. To evaluate this hypothesis, we tested two indirect but largely used markers of hypoxia that produced consistent findings in models of cerebral ischemia, namely pimonidazole and HIF-1 α (Bergeron et al. 1999; Weinstein et al. 2004; Noto et al. 2006, 2007; Thored et al. 2007; Schelshorn et al. 2009; Yeh et al. 2011; Yu et al. 2011). Additionally, we investigated another marker affected by hypoxia, HMGB1 (Faraco et al. 2007; Itoh et al. 2012). Although largely used as a marker of

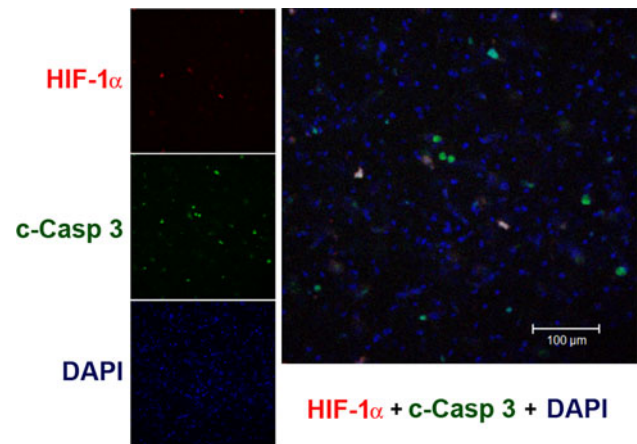


Fig. 8 Photomicrographs illustrating localization of hypoxia-inducible factor 1 α -positive (*HIF-1 α*) and the cleaved form of caspase 3 (*c-Casp 3*). Note that a subpopulation of cleaved caspase-3-immunopositive neurons, suggesting apoptosis in a human surgical specimen obtained from patient P6 (Table 2), affected by frontal lobe epilepsy, present with immunofluorescence for HIF-1 α . Scale bar, 100 μ m

hypoxia for tumors (Kizaka-Kondoh and Konse-Nagasawa 2009), pimonidazole was never tested before in the models of SE. At the earliest time intervals from SE, we observed three patterns of immunostaining: the first one consisted of diffuse immunoreactivity that did not identify specific cellular structures, present in various cerebral regions including the CA, which was reminiscent of the distribution of pimonidazole immunoreactivity in core lesions of rats exposed to cerebral ischemia (Noto et al. 2006, 2007; Thored et al. 2007). The second pattern, instead, consisted of previously unreported Golgi-like stained cells observed in various hippocampal and extrahippocampal regions. Finally, we also observed darkly stained neuronal somas in specific brain regions, including DR, IPR, and Tg, as also found in a model of cerebral malaria (Hempel et al. 2011). Intriguingly, pimonidazole-immunostained cells increased and became more diffuse by prolonging the duration of SE. A decrease in pimonidazole-immunostained cells occurred from 7 to 14 days, but these cells robustly reappeared at 21 days after SE induction when all animals had developed spontaneous recurrent seizures. These changes were especially evident in deep brain regions, such as DR, IPR, and PVH, a phenomenon that was at variance with the localization observed immediately after SE. Although we are unaware of the possible exposure of these regions to hypoxia, the strong labeling found in DR, IPR, and PVH is suggestive of putative sites of vulnerability in the presence of recurrent seizures.

In view of the ethical concerns related to pimonidazole administration in humans, we alternatively investigated the expression of HIF-1 α in brain samples obtained from patients treated by neurosurgical removal of the epileptic

focus. Cells immunoreactive to HIF-1 α were recently found in postmortem samples from patients affected by epilepsy (Feast et al. 2012). Interestingly, HIF-1 α immunoreactivity in pilocarpine-treated rats presenting with spontaneous seizures was found in all neurons immunopositive to pimonidazole. Neurons labeled by HIF-1 α antibodies were also found in patients affected by pharmacoresistance. Although we did not evaluate any control human sample, both for ethical and technical reasons, the absence of immunopositivity for HIF-1 α in control non-epileptic rats is suggestive of the induction of HIF-1 α in response to hypoxia. Exposure to hypoxia could take place during surgical removal of the epileptic focus or, alternatively, in vivo during exposure to recurrent seizures. Evidence of HIF-1 α - and pimonidazole-immunopositive neurons in the brain of rats suffering from recurrent seizures support the hypothesis that hypoxia could occur in vivo in relation to epileptic activity. In addition, the very limited expression of HIF-1 α in interneurons of human samples does not support a diffuse exposure of the surgical specimen to hypoxia.

The markers we used to identify the cell types presenting with immunoreactivity to pimonidazole identified NPY and somatostatin interneurons as immunopositive, whereas PV and CCK interneurons did not express the investigated marker of hypoxia. Several lines of evidence suggest that PV interneurons are deeply affected both in patients and in models of TLE (Kobayashi and Buckmaster 2003; Sayin et al. 2003; Arellano et al. 2004; Gorter et al. 2011; van Vliet et al. 2004). In addition to PV interneurons, NPY and somatostatin interneurons were also found to be partially lost in TLE, at least in the hilus of DG (Mathern et al. 1995; Sundstrom et al. 2001). In the experimental models of TLE, the loss of NPY and somatostatin interneurons has been consistently found in the hilus of DG (Sloviter 1987; Mitchell et al. 1995) and also in extrahippocampal regions (Bortel et al. 2010; Benini et al. 2011). Interestingly, interneurons were shown to be progressively reduced during epileptogenesis and this phenomenon was hypothesized to be associated with the appearance of spontaneous recurrent seizures (Gorter et al. 2011; van Vliet et al. 2004). Interneuron loss after intensive kindling was associated with the development of recurrent spontaneous seizures (Sayin et al. 2003). Thus, loss of interneurons appears to be a phenomenon involved in epileptogenesis, but mechanisms responsible for this cell loss are still not defined. Our data suggest that hypoxia occurs during seizures and could participate, at least in the case of NPY and somatostatin interneurons, in producing cell damage.

Interneurons identified by both PV and NPY antibodies were found to express HMGB1 cytoplasmic immunopositivity in patients affected by pharmacoresistant epilepsy.

HMGB1 is a nonhistone nuclear DNA-binding protein that is able to stabilize nucleosome formation and to preserve nuclear homeostasis (Hayakawa et al. 2010). Notably, HMGB1 is released to the cytoplasm and, then, secreted into the extracellular space from damaged or necrotic cells (Kim et al. 2006; Qiu et al. 2008). When released out of the cell, HMGB1 contributes to inflammation, proliferation, migration, and cell survival as well as to epileptic activity (Maroso et al. 2010). Thus, HMGB1 antibodies identified interneurons that were probably injured by unspecified mechanisms, which could be anyway related to epilepsy (Maroso et al. 2010) and ischemia (Kim et al. 2006; Qiu et al. 2008). In the case of NPY interneurons, the presence of HIF-1 α immunopositivity suggests that ischemia and/or hypoxia were possible factors involved in the changes of HMGB1 localization in cell compartments.

HIF-1 α is a major player of the cellular response to hypoxia and ischemia, as shown in models of stroke (Helton et al. 2005). In the presence of hypoxia, HIF-1 α is upregulated and mediates angiogenic and metabolic responses or, alternatively, cell death by activating different target genes (Semenza et al. 2000). An experiment on brain-specific knock-out of HIF-1 α demonstrated that decreasing the level of HIF-1 α can be neuroprotective (Helton et al. 2005). Further studies have consistently shown the elevation of HIF-1 α expression in hippocampus and cortex is associated with apoptotic neuronal loss after cerebral ischemia (Li et al. 2005). The findings on cleaved caspase-3 immunoreactivity in NPY interneurons could support the hypothesis that HIF-1 α is involved in mediating cell damage. Caspases are activated after seizure induction in rodents (Niquet et al. 2003) and their inhibition results in neuroprotection (Henshall and Simon 2005). Interestingly, caspase 3 was found to be upregulated and activated by cleavage in resected neocortex from patients affected by pharmacoresistant epilepsy (Henshall et al. 2000). Our findings raise the possibility that neurons undergoing cell death could be, at least in part, interneurons. Of these cells, at least NPY interneurons presented evidence of exposure to hypoxia both in patients and in rats suffering from recurrent seizures.

Ischemia and/or hypoxia are putative mechanisms of neuronal cell damage in epilepsy (Plum et al. 1968; Simon 1985; Fabene et al. 2007), which have received progressively poor attention after the discovery of excitotoxicity as the leading cause of seizure-associated cerebral injury (Siesjö et al. 1986; Meldrum 2002). In recent years, evidence accumulated to support a role for cerebral blood circulation in mediating damage in models of SE (Fabene et al. 2007; Biagini et al. 2008; Nnode-Ekane et al. 2010; Gualtieri et al. 2012) and in patients affected by pharmacoresistant epilepsy (Rigau et al. 2007; Mott et al. 2009). In particular, functional changes in cerebral blood flow were

shown to challenge the increased metabolic demand of hyperactive neurons in animal models of seizures and in patients (Ma et al. 2009; Zhao et al. 2009; Geneslaw et al. 2011). Our findings suggest that a subtle, cell-specific damage may occur in the brain exposed to recurrent seizures, mainly affecting a population of interneurons critically involved in controlling seizure activity. Importantly, repeated hypoxic seizure-related insults could explain the progressive course of some epileptic disorders like TLE with hippocampal sclerosis, in which neuropsychological and morphometric MRI studies have demonstrated chronic temporal and extra-temporal damage (Bernhardt et al. 2009; Coan et al. 2009). In the long term, this process could contribute to aggravate the course of epilepsy.

Acknowledgments This study was supported by the Emilia-Romagna Region (Region-University Program 2007–2009, grant 1232 to GB, SM, and PFN).

References

- Arellano, J. I., Muñoz, A., Ballesteros-Yáñez, I., Sola, R. G., & DeFelipe, J. (2004). Histopathology and reorganization of chandelier cells in the human epileptic sclerotic hippocampus. *Brain*, *127*, 45–64.
- Arteel, G. E., Thurman, R. G., & Raleigh, J. A. (1998). Reductive metabolism of the hypoxia marker pimonidazole is regulated by oxygen tension independent of the pyridine nucleotide redox state. *European Journal of Biochemistry*, *253*, 743–750.
- Arteel, G. E., Thurman, R. G., Yates, J. M., & Raleigh, J. A. (1995). Evidence that hypoxia markers detect oxygen gradients in liver: Pimonidazole and retrograde perfusion of rat liver. *British Journal of Cancer*, *72*, 889–895.
- Benini, R., Longo, D., Biagini, G., & Avoli, M. (2011). Perirhinal cortex hyperexcitability in pilocarpine-treated epileptic rats. *Hippocampus*, *21*, 702–713.
- Bergeron, M., Yu, A. Y., Solway, K. E., Semenza, G. L., & Sharp, F. R. (1999). Induction of hypoxia-inducible factor-1 (HIF-1) and its target genes following focal ischaemia in rat brain. *European Journal of Neuroscience*, *11*, 4159–4170.
- Bernhardt, B. C., Worsley, K. J., Kim, H., Evans, A. C., Bernasconi, A., & Bernasconi, N. (2009). Longitudinal and cross-sectional analysis of atrophy in pharmacoresistant temporal lobe epilepsy. *Neurology*, *72*, 1747–1754.
- Biagini, G., Baldelli, E., Longo, D., Contri, M. B., Guerrini, U., Sironi, L., et al. (2008). Proepileptic influence of a focal vascular lesion affecting entorhinal cortex-CA3 connections after status epilepticus. *Journal of Neuropathology and Experimental Neurology*, *67*, 687–701.
- Biagini, G., Baldelli, E., Longo, D., Pradelli, L., Zini, I., Rogawski, M. A., et al. (2006). Endogenous neurosteroids modulate epileptogenesis in a model of temporal lobe epilepsy. *Experimental Neurology*, *201*, 519–524.
- Biagini, G., D'Arcangelo, G., Baldelli, E., D'Antuono, M., Tancredi, V., & Avoli, M. (2005). Impaired activation of CA3 pyramidal neurons in the epileptic hippocampus. *NeuroMolecular Medicine*, *7*, 325–342.
- Biagini, G., Pich, E. M., Carani, C., Marrama, P., Gustafsson, J. A., Fuxe, K., et al. (1993). Indole-pyruvic acid, a tryptophan ketoanalogue, antagonizes the endocrine but not the behavioral effects of repeated stress in a model of depression. *Biological Psychiatry*, *33*, 712–719.
- Blümcke, I., Thom, M., Aronica, E., Armstrong, D. D., Vinters, H. V., Palmini, A., et al. (2011). The clinicopathologic spectrum of focal cortical dysplasias: a consensus classification proposed by an ad hoc Task Force of the ILAE Diagnostic Methods Commission. *Epilepsia*, *52*, 158–174.
- Bortel, A., Longo, D., de Guzman, P., Dubeau, F., Biagini, G., & Avoli, M. (2010). Selective changes in inhibition as determinants for limited hyperexcitability in the insular cortex of epileptic rats. *European Journal of Neuroscience*, *31*, 2014–2023.
- Cao, G., Pei, W., Lan, J., Stetler, R. A., Luo, Y., Nagayama, T., et al. (2001). Caspase activated DNase/DNA fragmentation factor 40 mediates apoptotic DNA fragmentation in transient cerebral ischemia and in neuronal cultures. *Journal of Neuroscience*, *21*, 4678–4690.
- Chen, C., Hu, Q., Yan, J., Lei, J., Qin, L., Shi, X., et al. (2007). Multiple effects of 2ME2 and D609 on the cortical expression of HIF-1 α and apoptotic genes in a middle cerebral artery occlusion-induced focal ischemia rat model. *Journal of Neurochemistry*, *102*, 1831–1841.
- Coan, A. C., Appenzeller, S., Bonilha, L., Li, L. M., & Cendes, F. (2009). Seizure frequency and lateralization affect progression of atrophy in temporal lobe epilepsy. *Neurology*, *73*, 834–842.
- Curia, G., Longo, D., Biagini, G., Jones, R. S., & Avoli, M. (2008). The pilocarpine model of temporal lobe epilepsy. *Journal of Neuroscience Methods*, *172*, 143–157.
- Fabene, P. F., Merigo, F., Galiè, M., Benati, D., Bernardi, P., Farace, P., et al. (2007). Pilocarpine-induced status epilepticus in rats involves ischemic and excitotoxic mechanisms. *PLoS ONE*, *2*, e1105.
- Faraco, G., Fossati, S., Bianchi, M. E., Patrone, M., Pedrazzi, M., Sparatore, B., et al. (2007). High mobility group box 1 protein is released by neural cells upon different stresses and worsens ischemic neurodegeneration in vitro and in vivo. *Journal of Neurochemistry*, *103*, 590–603.
- Feast, A., Martinian, L., Liu, J., Catarino, C. B., Thom, M., & Sisodiya, S. M. (2012). Investigation of hypoxia-inducible factor-1 α in hippocampal sclerosis: A postmortem study. *Epilepsia*, *53*, 1349–1359.
- Geneslaw, A. S., Zhao, M., Ma, H., & Schwartz, T. H. (2011). Tissue hypoxia correlates with intensity of interictal spikes. *Journal of Cerebral Blood Flow and Metabolism*, *31*, 1394–1402.
- Gorter, J. A., van Vliet, E. A., Aronica, E., & Lopes da Silva, F. H. (2011). Progression of spontaneous seizures after status epilepticus is associated with mossy fibre sprouting and extensive bilateral loss of hilar parvalbumin and somatostatin-immunoreactive neurons. *European Journal of Neuroscience*, *13*, 657–669.
- Gualtieri, F., Curia, G., Marinelli, C., & Biagini, G. (2012). Increased perivascular laminin predicts damage to astrocytes in CA3 and piriform cortex following chemoconvulsive treatments. *Neuroscience*, *218*, 278–294.
- Hayakawa, K., Qiu, J., & Lo, E. H. (2010). Biphasic actions of HMGB1 signaling in inflammation and recovery after stroke. *Annals of the New York Academy of Sciences*, *1207*, 50–57.
- Helton, R., Cui, J., Scheel, J. R., Ellison, J. A., Ames, C., Gibson, C., et al. (2005). Brain-specific knock-out of hypoxia-inducible factor-1 α reduces rather than increases hypoxic-ischemic damage. *Journal of Neuroscience*, *25*, 4099–4107.
- Hempel, C., Combes, V., Hunt, N. H., Kurtzhals, J. A., & Grau, G. E. (2011). CNS hypoxia is more pronounced in murine cerebral than noncerebral malaria and is reversed by erythropoietin. *American Journal of Pathology*, *179*, 1939–1950.
- Henshall, D. C., Clark, R. S., Adelson, P. D., Chen, M., Watkins, S. C., & Simon, R. P. (2000). Alterations in bcl-2 and caspase gene

- family protein expression in human temporal lobe epilepsy. *Neurology*, 55, 250–257.
- Henshall, D. C., & Simon, R. P. (2005). Epilepsy and apoptosis pathways. *Journal of Cerebral Blood Flow and Metabolism*, 25, 1557–1572.
- Hossain, M. A. (2005). Molecular mediators of hypoxic-ischemic injury and implications for epilepsy in the developing brain. *Epilepsy & Behavior*, 7, 204–213.
- Hota, K. B., Hota, S. K., Srivastava, R. B., & Singh, S. B. (2012). Neuroglobin regulates hypoxic response of neuronal cells through Hif-1 α - and Nrf2-mediated mechanism. *Journal of Cerebral Blood Flow and Metabolism*, 32, 1046–1060.
- Ingvar, M. (1986). Cerebral blood flow and metabolic rate during seizures. Relationship to epileptic brain damage. *Annals of the New York Academy of Sciences*, 462, 194–206.
- Itoh, T., Takita, M., Sorelle, J. A., Sugimoto, K., Chujo, D., Qin, H., et al. (2012). Correlation of released HMGB1 levels with the degree of islet damage in mice and humans and with the outcomes of islet transplantation in mice. *Cell Transplantation*. doi:10.37271/096368912X640592.
- Kim, J. B., Sig Choi, J., Yu, Y. M., Nam, K., Piao, C. S., Kim, S. W., et al. (2006). HMGB1, a novel cytokine-like mediator linking acute neuronal death and delayed neuroinflammation in the postischemic brain. *Journal of Neuroscience*, 26, 6413–6421.
- Kizaka-Kondoh, S., & Konse-Nagasawa, H. (2009). Significance of nitroimidazole compounds and hypoxia-inducible factor-1 for imaging tumor hypoxia. *Cancer Science*, 100, 1366–1373.
- Kobayashi, M., & Buckmaster, P. S. (2003). Reduced inhibition of dentate granule cells in a model of temporal lobe epilepsy. *Journal of Neuroscience*, 23, 2440–2452.
- Kreisman, N. R., Magee, J. C., & Brizzee, B. L. (1991). Relative hypoperfusion in rat cerebral cortex during recurrent seizures. *Journal of Cerebral Blood Flow and Metabolism*, 11, 77–87.
- Li, L., Qu, Y., Li, J., Xiong, Y., Mao, M., & Mu, D. (2007). Relationship between HIF-1 α expression and neuronal apoptosis in neonatal rats with hypoxia-ischemia brain injury. *Brain Research*, 1180, 133–139.
- Li, Y., Zhou, C., Calvert, J. W., Colohan, A. R., & Zhang, J. H. (2005). Multiple effects hyperbaric oxygen on the expression of HIF-1 α and apoptotic genes in a global ischemia-hypotension rat model. *Experimental Neurology*, 191, 198–210.
- Ma, H., Geneslaw, A., Zhao, M., Suh, M., Perry, C., & Schwartz, T. H. (2009). The importance of latency in the focality of perfusion and oxygenation changes associated with triggered afterdischarges in human cortex. *Journal of Cerebral Blood Flow and Metabolism*, 29, 1003–1014.
- Maroso, M., Balosso, S., Ravizza, T., Liu, J., Aronica, E., Iyer, A. M., et al. (2010). Toll-like receptor 4 and high-mobility group box-1 are involved in ictogenesis and can be targeted to reduce seizures. *Nature Medicine*, 16, 413–419.
- Mathern, G. W., Babb, T. L., Pretorius, J. K., & Leite, J. P. (1995). Reactive synaptogenesis and neuron densities for neuropeptide Y, somatostatin, and glutamate decarboxylase immunoreactivity in the epileptogenic human fascia dentata. *Journal of Neuroscience*, 15, 3990–4004.
- Meldrum, B. S. (2002). Concept of activity-induced cell death in epilepsy: Historical and contemporary perspectives. *Progress in Brain Research*, 135, 3–11.
- Meldrum, B. S., & Nilsson, B. (1976). Cerebral blood flow and metabolic rate early and late in prolonged epileptic seizures induced in rats by bicuculline. *Brain*, 99, 523–542.
- Mitchell, J., Gatherer, M., & Sundstrom, L. E. (1995). Loss of hilar somatostatin neurons following tetanus toxin-induced seizures. *Acta Neuropathologica*, 89, 425–430.
- Mott, R. T., Thore, C. R., Moody, D. M., Glazier, S. S., Ellis, T. L., & Brown, W. R. (2009). Reduced ratio of afferent to total vascular density in mesial temporal sclerosis. *Journal of Neuropathology and Experimental Neurology*, 68, 1147–1154.
- Ndode-Ekane, X. E., Hayward, N., Gröhn, O., & Pitkänen, A. (2010). Vascular changes in epilepsy: functional consequences and association with network plasticity in pilocarpine-induced experimental epilepsy. *Neuroscience*, 166, 312–332.
- Nevander, G., Ingvar, M., Auer, R., & Siesjö, B. K. (1985). Status epilepticus in well-oxygenated rats causes neuronal necrosis. *Annals of Neurology*, 18, 281–290.
- Niquet, J., Baldwin, R. A., Allen, S. G., Fujikawa, D. G., & Wasterlain, C. G. (2003). Hypoxic neuronal necrosis: Protein synthesis-independent activation of a cell death program. *Proceedings of the National Academy of Sciences of the United States of America*, 100, 2825–2830.
- Northington, F. J., Chavez-Valdez, R., & Martin, L. J. (2011). Neuronal cell death in neonatal hypoxia-ischemia. *Annals of Neurology*, 69, 743–758.
- Noto, T., Furuichi, Y., Ishiye, M., Matsuoka, N., Aramori, I., Mutoh, S., et al. (2006). Temporal and topographic profiles of tissue hypoxia following transient focal cerebral ischemia in rats. *Journal of Veterinary Medicine Science*, 68, 803–807.
- Noto, T., Furuichi, Y., Ishiye, M., Matsuoka, N., Aramori, I., Mutoh, S., et al. (2007). Tacrolimus (FK506) limits accumulation of granulocytes and platelets and protects against brain damage after transient focal cerebral ischemia in rat. *Biology and Pharmaceutical Bulletin*, 30, 313–317.
- Plum, F., Posner, J. B., & Troy, B. (1968). Cerebral metabolic and circulatory responses to induced convulsions in animals. *Archives of Neurology*, 18, 1–13.
- Qiu, J., Nishimura, M., Wang, Y., Sims, J. R., Qiu, S., Savitz, S. I., et al. (2008). Early release of HMGB-1 from neurons after the onset of brain ischemia. *Journal of Cerebral Blood Flow and Metabolism*, 28, 927–938.
- Racine, R. J. (1972). Modification of seizure activity by electrical stimulation. II. Motor seizure. *Electroencephalography and Clinical Neurophysiology*, 32, 281–294.
- Rademakers, S. E., Lok, J., van der Kogel, A. J., Bussink, J., & Kaanders, J. H. (2011). Metabolic markers in relation to hypoxia; staining patterns and colocalization of pimonidazole, HIF-1 α , CAIX, LDH-5, GLUT-1, MCT1 and MCT4. *BMC Cancer*, 11, 167.
- Rigau, V., Morin, M., Rousset, M. C., de Bock, F., Lebrun, A., Coubes, P., et al. (2007). Angiogenesis is associated with blood-brain barrier permeability in temporal lobe epilepsy. *Brain*, 130, 1942–1956.
- Saunders, M. I., Anderson, P. J., Bennett, M. H., Dische, S., Minchinton, A. I., & Stratford, M. R. L. (1984). The clinical testing of Ro 03–8799—Pharmacokinetics, toxicology, tissue and tumor concentrations. *International Journal of Radiation Oncology Biology Physics*, 10, 1759–1763.
- Sayin, U., Osting, S., Hagen, J., Rutecki, P., & Sutula, T. (2003). Spontaneous seizures and loss of axo-axonic and axo-somatic inhibition induced by repeated brief seizures in kindled rats. *Journal of Neuroscience*, 23, 2759–2768.
- Scaffidi, P., Misteli, T., & Bianchi, M. E. (2002). Release of chromatin protein HMGB1 by necrotic cells triggers inflammation. *Nature*, 418, 191–195.
- Schelshorn, D. W., Schneider, A., Kuschinsky, W., Weber, D., Krüger, C., Dittgen, T., et al. (2009). Expression of hemoglobin in rodent neurons. *Journal of Cerebral Blood Flow and Metabolism*, 29, 585–595.
- Schindler, C. K., Pearson, E. G., Bonner, H. P., So, N. K., Simon, R. P., Prehn, J. H., et al. (2006). Caspase-3 cleavage and nuclear localization of caspase-activated DNase in human temporal lobe epilepsy. *Journal of Cerebral Blood Flow and Metabolism*, 26, 583–589.

- Semenza, G. L. (2011). Hypoxia. Cross talk between oxygen sensing and the cell cycle machinery. *American Journal of Physiology-Cell Physiology*, 301, C550–C552.
- Semenza, G. L., Agani, F., Feldser, D., Iyer, N., Kotch, L., Laughner, E., et al. (2000). Hypoxia, HIF-1, and the pathophysiology of common human diseases. *Advances in Experimental Medicine and Biology*, 475, 123–130.
- Siesjö, B. K., Ingvar, M., & Wieloch, T. (1986). Cellular and molecular events underlying epileptic brain damage. *Annals of the New York Academy of Sciences*, 462, 207–223.
- Simon, R. P. (1985). Physiologic consequences of status epilepticus. *Epilepsia*, 26(Suppl 1), S58–S66.
- Sloviter, R. S. (1987). Decreased hippocampal inhibition and a selective loss of interneurons in experimental epilepsy. *Science*, 235, 73–76.
- Sundstrom, L. E., Brana, C., Gatherer, M., Mephram, J., & Rougier, A. (2001). Somatostatin- and neuropeptide Y-synthesizing neurones in the fascia dentata of humans with temporal lobe epilepsy. *Brain*, 124, 688–697.
- Thored, P., Wood, J., Arvidsson, A., Cammenga, J., Kokaia, Z., & Lindvall, O. (2007). Long-term neuroblast migration along blood vessels in an area with transient angiogenesis and increased vascularization after stroke. *Stroke*, 38, 3032–3039.
- van Vliet, E. A., Aronica, E., Tolner, E. A., Lopes da Silva, F. H., & Gorter, J. A. (2004). Progression of temporal lobe epilepsy in the rat is associated with immunocytochemical changes in inhibitory interneurons in specific regions of the hippocampal formation. *Experimental Neurology*, 187, 367–379.
- Weinstein, P. R., Hong, S., & Sharp, F. R. (2004). Molecular identification of the ischemic penumbra. *Stroke*, 35(11 Suppl 1), 2666–2670.
- Yang, Q. W., Xiang, J., Zhou, Y., Zhong, Q., & Li, J. C. (2010). Targeting HMGB1/TLR4 signaling as a novel approach to treatment of cerebral ischemia. *Frontiers in Bioscience*, 2, 1081–1091.
- Yeh, S. H., Ou, L. C., Gean, P. W., Hung, J. J., & Chang, W. C. (2011). Selective inhibition of early—But not late—Expressed HIF-1 α is neuroprotective in rats after focal ischemic brain damage. *Brain Pathology*, 21, 249–262.
- Yu, C. H., Moon, C. T., Sur, J. H., Chun, Y. I., Choi, W. H., & Yhee, J. Y. (2011). Serial expression of hypoxia inducible factor-1 α and neuronal apoptosis in hippocampus of rats with chronic ischemic brain. *Journal of Korean Neurosurgical Society*, 50, 481–485.
- Zhao, M., Ma, H., Suh, M., & Schwartz, T. H. (2009). Spatiotemporal dynamics of perfusion and oximetry during ictal discharges in the rat neocortex. *Journal of Neuroscience*, 29, 2814–2823.